Approximations for the treatment of final state interactions in nuclear knockout form factors

F. Cannata
Dipartimento di Fisica and Istituto Nazionale di Fisica Nucleare, I-40126 Bologna, Italy

J. P. Dedonder*
Division de Physique Théorique, Institut de Physique Nucléaire, F-91406 Orsay, Cedex, France and Laboratoire de Physique Nucléaire, Université Paris VII, Paris, France

L. Lesniak
Department of Theoretical Physics, Institute of Nuclear Physics, Radzikowskiego 152, PL-31342 Krakow, Poland

(Received 26 July 1985)

To investigate the role of final state interactions in knockout reactions, we study the transition form factor corresponding to the absorption of a scalar probe in a single particle model description of the nucleus. The numerical aspects of an approximation which treats at the same level initial and final state interactions are discussed. It provides fair agreement with the corresponding exact calculations for momenta of the ejected nucleon larger than 2 fm^{-1}. Comparisons with various other approximations show that a careful treatment of the final state interaction is necessary to obtain a realistic estimate of the form factor.

I. INTRODUCTION

It is well known that the study of nuclear momentum distributions by knockout reactions requires an accurate calculation of final state interaction (FSI) effects between the ejected nucleon and the residual nucleus. At the present moment, however, there is still a rather unbalanced treatment between the rather sophisticated initial state interaction (introduction of short-range correlations, tensor correlations, etc.) and the rather crude treatment of the final state distortion. In fact, the optical potential describing the FSI requires for consistency the same microscopic ingredients as the initial state interaction. It should contain the same dynamics as the ground state in order to respect the unitarity of the theory.[1] In a realistic calculation the short-range correlations are related to n-particle—n-hole excitations in the ground state. Taking into account the corresponding nuclear states in the final state interaction requires one to consider the coupling of the various channels for the residual nucleus. In a one-channel model this can be described by a complex energy dependent optical potential. Phenomenologically this optical potential generates globally not only a reduction of strength due to excitations of other channels but also an enhancement of the large momentum transfer region (relative to a plane-wave approximation) since large momentum transfers can be generated by successive scatterings with relatively low momentum transfer, thereby not probing the high Fourier components of the bound state wave function. While the effects due to the coupling of the channels have been studied by Haider and Londergan,[2] we explore, here, essentially the second aspect.

What has been found in general from phenomenological calculations is an increase of high momentum Fourier components due to short-range correlations. We show here in a rather schematic model where the dynamics is, however, treated consistently (i.e., we have the same potential responsible for the binding and for the FSI), that equivalent effects, i.e., deviations from a shell model plane-wave result, can be due to FSI effects and not necessarily to short-range correlations. In order to show the sensitivity of the results to a good treatment of FSI, we display also various approximate results which show how delicate it is to make approximations on FSI.

Recently[3,4] a high energy approximation for the nucleon knockout transition form factor has been proposed. The nucleon was considered to be ejected by the scalar projectile and its interaction in the final state with the residual nucleus was described by the same potential responsible for the binding. In the calculation of the approximate transition matrix element only the initial single particle bound state wave function and the potential enter but not the final state continuum wave function.

The approximate form factor respects orthogonality in the sense that for $\mathbf{q}\rightarrow 0$ it vanishes (orthogonality of initial bound state and final continuum state).[5] The high nucleon momentum $|\mathbf{k}|$ and small momentum transfer limit $|\mathbf{q}|$ have been discussed in Ref. 4. (See Fig. 1.)

In realistic cases like (e,e'p) reactions[6] most nucleons are ejected with momentum $\mathbf{k}$ close to $\mathbf{q}$. Moreover, the data are taken at intermediate energies which limit both $|\mathbf{q}|$ and $|\mathbf{k}|$ values to a few hundred MeV/c. In order to test the accuracy of the approximation[3] in this new regime we present the results for the $1s$ and $1p$ form factors calculated exactly and in the approximate way for the Woods-Saxon and the square well potentials; a compar-

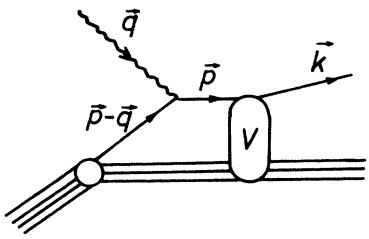

FIG. 1. Representation of the knockout form factor. The momentum of the ejected nucleon is represented by **k**, while **q** denotes the momentum transfer to the nucleus.

ison is also made with the plane-wave approximation. Section II is devoted to the presentation of various approximations for the treatment of the final state interaction. In Sec. III, we present detailed numerical comparisons of the transition form factors. Finally in Sec. IV we summarize and discuss the present study.

II. APPROXIMATIONS FOR THE TRANSITION FORM FACTOR

The transition nuclear form factor for the nucleon knockout from an initial state $\varphi_{LM}(\mathbf{r})$ with angular momentum L and projection M reads:

$$S_{LM}(\mathbf{k},\mathbf{q})=\int d^3r\,\psi_{\mathbf{k}}^{(-)*}(\mathbf{r})e^{i\mathbf{q}\cdot\mathbf{r}}\varphi_{LM}(\mathbf{r})\ . \tag{1}$$

The scattering wave function $\psi_{\mathbf{k}}^{(-)}(\mathbf{r})$ is the solution of the Schrödinger equation

$$H\psi_{\mathbf{k}}^{(-)}(\mathbf{r})=E_k\psi_{\mathbf{k}}^{(-)}(\mathbf{r})\ , \tag{2}$$

where H is the single particle Hamiltonian

$$H=-\frac{\nabla^2}{2m_{\mathrm{N}}}+V(\mathbf{r}) \tag{3}$$

of the nucleon having a mass m_{N} and the final kinetic energy $E_k=k^2/2m_{\mathrm{N}}$. In the absence of the final state interaction the scattering wave reduces to the plane wave

$$\chi_{\mathbf{k}}(\mathbf{r})=e^{i\mathbf{k}\cdot\mathbf{r}}\ . \tag{4}$$

The plane-wave approximation for the form factor

$$\phi_{LM}(\mathbf{k}-\mathbf{q})=\int d^3r\,e^{-i(\mathbf{k}-\mathbf{q})\cdot\mathbf{r}}\varphi_{LM}(\mathbf{r}) \tag{5}$$

is the Fourier transform of the initial bound state. This function satisfies the Schrödinger equation with the *same* Hamiltonian:

$$H\varphi_{LM}(\mathbf{r})=\epsilon_{LM}\varphi_{LM}(\mathbf{r})\ , \tag{6}$$

where ϵ_{LM} are the binding (negative) energies.

The transition form factor can always be decomposed as the sum of the plane-wave form factor (5) and a correction $A_{LM}(\mathbf{k},\mathbf{q})$ which embodies the final state distortion and ensures the orthogonality property

$$S_{LM}(\mathbf{k},\mathbf{q})=\phi_{LM}(\mathbf{k}-\mathbf{q})+A_{LM}(\mathbf{k},\mathbf{q})\ , \tag{7}$$

where

$$A_{LM}(\mathbf{k},\mathbf{q})=\int\frac{d^3p}{(2\pi)^3}\langle\chi_{\mathbf{k}}\,|\,V\,|\,\mathbf{p}\rangle\langle\mathbf{p}\,|\,G_+(E_k)O_{\mathbf{q}}\,|\,\varphi_{LM}\rangle\ . \tag{8}$$

In Eq. (8), the transition operator is

$$O_{\mathbf{q}}=e^{i\mathbf{q}\cdot\mathbf{r}} \tag{9}$$

and the interacting Green's function reads

$$G_+(E_k)=(E_k+i\delta-H)^{-1}\ . \tag{10}$$

The approximation we intend to investigate in the following has been developed in Refs. 3 and 4. It consists of replacing the matrix element of the Green's operator in Eq. (8) by an approximate one which takes into account the effective energy of the nucleon once the probe has been absorbed. This approximation makes the Green's operator entering (8) diagonal in momentum space and the correction term $A_{LM}(\mathbf{k},\mathbf{q})$ becomes

$$A_{LM}^{\mathrm{appr}}(\mathbf{k},\mathbf{q})=\int\frac{d^3p}{(2\pi)^3}\frac{V(\mathbf{p}-\mathbf{k})\phi_{LM}(\mathbf{p}-\mathbf{q})}{E_k+i\delta+\dfrac{(\mathbf{p}-\mathbf{q})^2-\mathbf{p}^2}{2m_{\mathrm{N}}}-\epsilon_{LM}}\ , \tag{11}$$

where

$$V(\mathbf{p})=\int d^3r\,e^{-i\mathbf{p}\cdot\mathbf{r}}V(\mathbf{r})\ . \tag{12}$$

By shifting the integration variable $\mathbf{p}$ in (11) we obtain:

$$A_{LM}^{\mathrm{appr}}(\mathbf{k},\mathbf{q})=\int\frac{d^3p}{(2\pi)^3}\frac{V(\mathbf{p}+\mathbf{q}-\mathbf{k})\phi_{LM}(\mathbf{p})}{E_k+i\delta-\dfrac{q^2}{2m_{\mathrm{N}}}-\epsilon_{LM}-\dfrac{\mathbf{p}\cdot\mathbf{q}}{m_{\mathrm{N}}}}\ . \tag{13}$$

Since the bound state wave function $\phi_{LM}(\mathbf{p})$ [Eq. (5)] can be written as the product of a radial wave function $\chi_L(p)$ and a spherical harmonic $Y_L^M(\hat{\mathbf{p}})$,

$$\phi_{LM}(\mathbf{p})=\chi_L(p)Y_L^M(\hat{\mathbf{p}}) \tag{14}$$

with $\hat{\mathbf{p}}=\mathbf{p}/p$, we arrive, upon using Eq. (12), at the following expression, for a central potential $V(\mathbf{r})=V(r)$:

$$A_{LM}^{\mathrm{appr}}(\mathbf{k},\mathbf{q})=\frac{2}{\pi}\sum_{lm}Y_l^{m*}(\hat{\mathbf{k}-\mathbf{q}})\int_0^\infty p^2dp\,\chi_L(p)G_l(p,|\,\mathbf{k}-\mathbf{q}\,|\,)\int d\hat{\mathbf{p}}\frac{Y_l^m(\hat{\mathbf{p}})Y_L^M(\hat{\mathbf{p}})}{E_k+i\delta-\dfrac{q^2}{2m_{\mathrm{N}}}-\epsilon_{LM}-\dfrac{\mathbf{p}\cdot\mathbf{q}}{m_{\mathrm{N}}}}\ . \tag{15}$$

In Eq. (15) the function $G_l(p, |\mathbf{k}-\mathbf{q}|)$ is given by the radial integral

$$G_l(p, |\mathbf{k}-\mathbf{q}|)=\int_0^\infty r^2 dr\, j_l(pr) j_l(|\mathbf{k}-\mathbf{q}|r) V(r) , \tag{16}$$

where $j_l(x)$ denotes the lth-order spherical Bessel function. We introduce the notation

$$\begin{bmatrix} l & L & \lambda \\ m & M & \mu \end{bmatrix} = [(2l+1)(2L+1)(2\lambda+1)]^{1/2} \times \begin{bmatrix} l & L & \lambda \\ m & M & \mu \end{bmatrix} \begin{bmatrix} l & L & \lambda \\ 0 & 0 & 0 \end{bmatrix} , \tag{17}$$

where the 3-j are defined as in Ref. 7. Choosing the quantization axis along the $\mathbf{q}$ direction, the angular integration in Eq. (15) is performed and yields

$$\int d\hat{\mathbf{p}} \frac{Y_l^m(\hat{\mathbf{p}}) Y_L^M(\hat{\mathbf{p}})}{E_k + i\delta - \frac{q^2}{2m_N} - \epsilon_{LM} - \frac{\mathbf{p}\cdot\mathbf{q}}{m_N}} = \frac{m_N}{pq} \sum_\lambda (2l+1)^2 \begin{bmatrix} l & L & \lambda \\ m & M & 0 \end{bmatrix} \left[Q_\lambda(z) - i\frac{\pi}{2}\theta(1-|z|) P_\lambda(z) \right] . \tag{18}$$

The step function is represented by the symbol θ while $P_\lambda(z)$ and $Q_\lambda(z)$ are, respectively, the Legendre polynomials and the second kind of Legendre functions.[8] Finally, the variable z introduced in Eq. (18) is defined as

$$z=\frac{k^2-q^2+2m_N|\epsilon_{LM}|}{2pq} .$$

Then the correction term (15) is expressed as

$$A_{LM}^{\text{appr}}(\mathbf{k},\mathbf{q}) = \frac{2m_N}{pq} \sum_{l,\lambda} (2\lambda+1)^{1/2} \begin{bmatrix} l & L & \lambda \\ -M & M & 0 \end{bmatrix} Y_l^{-M*}(\widehat{\mathbf{k}-\mathbf{q}}) \times \int_0^\infty p\, dp\, \chi_L(p) G_l(p, |\mathbf{k}-\mathbf{q}|) \left[Q_\lambda(z) - i\frac{\pi}{2}\theta(1-|z|) P_\lambda(z) \right] . \tag{19}$$

For comparison, we now write the partial wave expansion of the exact transition form factor given in Eq. (1). The ingoing scattering state reads

$$\psi_{\mathbf{k}}^{(-)}(\mathbf{r}) = 4\pi \sum_{lm} i^l e^{-i\delta_l} u_l(k,r) Y_l^m(\hat{\mathbf{r}}) Y_l^{m*}(\hat{\mathbf{k}}) , \tag{20}$$

where the phase shifts are denoted by δ_l. The (real) scattering waves $u_l(k,r)$ are the regular solutions of the Schrödinger equation which are asymptotically equal to $\sin[kr - l(\pi/2) + \delta_l]/kr$. Hence the form factor (1) is given by

$$S_{LM}(\mathbf{k},\mathbf{q}) = (4\pi)^{3/2} \sum_{lm,\lambda\mu} i^{\lambda-l} e^{i\delta_l} \begin{bmatrix} l & L & \lambda \\ m & M & \mu \end{bmatrix} \times K_{lL\lambda}(k,q) Y_l^{m*}(\hat{\mathbf{k}}) Y_\lambda^{\mu*}(\hat{\mathbf{q}}) \tag{21}$$

with the radial integral:

$$K_{lL\lambda}(k,q) = \int_0^\infty r^2 dr\, u_l(k,r) \chi_L(r) j_\lambda(qr) .$$

We note that the structure of the exact form factor (21) obviously respects Watson's theorem on final state interactions.[9]

At this point, we recall that the approximate form (13) which leads to (19) has been derived in Ref. 3 assuming k and q large compared to the Fermi momentum and, in principle, for small $|\mathbf{k}-\mathbf{q}|$. The comparison with the exact calculation in Sec. III will show that the restriction on $|\mathbf{k}-\mathbf{q}|$ is not severe and the approximation still yields fair agreement for values of $|\mathbf{k}-\mathbf{q}|$ as large as 4 fm^{-1}.

In Ref. 4, it has been shown that Eq. (13) should also hold in the high energy approximation for small momentum transfers, i.e., small q and large k. Indeed, as such the approximation is all right for q less than $1/c$ where c is a measure of the nuclear radius. We now see, however, from Eq. (19) that the imaginary part of the correction A_{LM}^{appr} arises from values of the intermediate momentum p in Eq. (15) larger than a minimal value

$$p_{\min} = \frac{k^2-q^2+2m_N|\epsilon_{LM}|}{2q}$$

which goes to infinity as q goes to zero, independently of k. This is in contradiction with Watson's theorem[9] and with the exact result. In fact the phase shift δ_l goes to zero in the large k limit independently of q. The approximation (19) can thus be used in the very small q region only when k is very large. The approximation can be improved by studying higher order corrections which would regenerate the missing imaginary part.

Returning now to the exact expression (21) for the transition form factor, we have chosen, as before, the direction of the momentum transfer, $\mathbf{q}$, as the angular momentum quantization axis. The plane-wave contribution is calculated directly via the Schrödinger equation and, in the numerical studies, the exact expression (21) is evaluated via a partial wave expansion of the difference between the exact form factor and the plane-wave contribution which improves the convergence.

The partial wave expansions (21) and (19) (which have to be added to the plane-wave contribution) are somehow different in nature. If (21) depends explicitly on both $\hat{\mathbf{k}}$

and $\hat{\mathbf{q}}$, (19) only depends on the direction $\mathbf{k}\hat{-}\mathbf{q}$. In the limit $|\mathbf{k}-\mathbf{q}|$ small as compared to k and q, very few terms contribute in the expansion (19), as is exemplified by the limit $\mathbf{k}=\mathbf{q}$ where one single term survives. In any case, the number of terms needed to evaluate (21) is at least twice as large as that used in calculating (19). Before we discuss in detail the results of the approximation (19) and, so as to display the sensitivity of the knockout form factors to the treatment of FSI, we briefly discuss some other commonly used approximations.

The on shell approximation is mainly used in cascade calculations.[10] It can be introduced by reexpressing Eq. (8) in terms of the elastic nucleon-nucleon scattering amplitude which fulfills the equation

$$t(E_k)=V+VG_+(E_k)V\ ,$$

and using the formal identity

$$t(E_k)G_0^+(E_k)=VG_+(E_k)\ ,$$

where $G_0^+(E_k)$ is the free Green's operator. Hence the correction term (8) reads

$$A_{LM}(\mathbf{k},\mathbf{q})=\int\frac{d^3p}{(2\pi)^3}\frac{\langle\chi_{\mathbf{k}}|t(E_k)|\mathbf{p}\rangle}{E_k+i\delta-\dfrac{\mathbf{p}^2}{2m_{\mathrm{N}}}}\phi_{LM}(\mathbf{p}-\mathbf{q})\ , \tag{22}$$

where $\langle\mathbf{k}|t(E_k)|\mathbf{p}\rangle$ represents the half-shell scattering matrix element. Now, in the on shell approximation one only retains the δ contribution of the Green's operator

$$A_{LM}^{\text{on shell}}(\mathbf{k},\mathbf{q})=-\frac{ikm_{\mathrm{N}}}{8\pi^2}\int d\hat{\mathbf{k}}'\langle\chi_{\mathbf{k}}|t(E_k)|\mathbf{k}'\rangle\phi_{LM}(\mathbf{k}'-\mathbf{q}) \tag{23}$$

(where $|\mathbf{k}'|=|\mathbf{k}|$) so that the fully on shell elastic scattering matrix element enters. Upon performing a partial wave expansion of the plane wave, we obtain (we consider an s wave bound state for simplicity)

$$\phi_{00}(\mathbf{k}-\mathbf{q})=4\pi\sum_{l=0}^{\infty}(2l+1)f_l(k,q)P_l(\hat{\mathbf{k}}\cdot\hat{\mathbf{q}}) \tag{24}$$

where

$$f_l(k,q)=\int_0^{\infty}r^2dr\,j_l(kr)j_l(qr)\varphi_{00}(r)\ . \tag{25}$$

Introducing then the partial wave expansion of the scattering amplitude, Eq. (23) is transformed to

$$A_{00}^{\text{on shell}}(\mathbf{k},\mathbf{q})=4i\pi\sum_{l=0}^{\infty}(2l+1)e^{i\delta_l}\sin\delta_l f_l(k,q)P_l(\mathbf{k}\cdot\mathbf{q})\ , \tag{26}$$

and the on shell transition form factor correspondingly reads

$$S_{00}^{\text{on shell}}(\mathbf{k},\mathbf{q})=4\pi\sum_{l=0}^{\infty}(2l+1)e^{i\delta_l}\cos\delta_l f_l(k,q)P_l(\hat{\mathbf{k}}\cdot\hat{\mathbf{q}})\ . \tag{27}$$

For the sake of completeness[11] and in view of the energies and momenta involved in the knockout reactions, one could think of introducing the eikonal approximation for the ingoing scattering state in Eq. (1). The correction to the plane-wave contribution would then read

$$A_{LM}^{\text{eik}}(\mathbf{k},\mathbf{q})=\int d^2b\,e^{-i(\mathbf{k}-\mathbf{q})\cdot\mathbf{b}}\int_{-\infty}^{\infty}dz\,\varphi_{LM}(\mathbf{b},z)(e^{-(i/\hbar v)\int_z^{\infty}V(\mathbf{b},z')dz'}-1)\ , \tag{28}$$

where v denotes the velocity of the ejected nucleon. In Eq. (28) we have assumed the quantization axis to be along the ejected momentum direction, $\hat{\mathbf{k}}$, and the vector $\mathbf{k}-\mathbf{q}$ to be approximately orthogonal to this direction which is reasonable in the high energy limit. One could easily take into account the longitudinal part of the vector $\mathbf{k}-\mathbf{q}$ and this may lead to appreciable modifications of the correction (28). We do not investigate here this contribution.

III. DISCUSSION OF THE RESULTS

The main aim of this section is to study the accuracy of the approximation (19) for the transition form factor given by Eq. (7) at intermediate energies when the ejected nucleon momenta are of the order of 2 to 4 fm^{-1}. We therefore compute numerically the exact transition form factor (21) and compare the results with those obtained with Eqs. (7) and (19) as well as with those arising from Eqs. (27) and (28).

The calculations have been performed for the spherical square well potential

$$V(r)=-V_0\quad r\le c\ ,$$
$$V(r)=0\quad r>c\ , \tag{29}$$

and for the Woods-Saxon potential

$$V(r)=-V_0(1+e^{(r-c/\beta)})^{-1}\ . \tag{30}$$

This allows one to study the influence of the diffuseness of the nuclear surface since the square well (29) may be considered as the limit of the potential (30) when the parameter β (fixed in the following calculations at the value $\beta=0.5$ fm) goes to zero. We have indeed checked numerically that the results obtained for the Woods-Saxon potential (29) go smoothly to the square well results with β decreasing to zero.

The depth, V_0, was fixed in both cases to the value $V_0=46.06$ MeV and the radius to $c=3$ fm. These parameters are relevant for the scattering on a light nucleus like carbon. Two single-particle bound states have been studied: $l=0$ ($1s$) and $l=1$ ($1p$) states.[12]

Let us first discuss the quasifree kinematical limit when the outgoing nucleon momentum k is equal to the momentum transfer q. We allow, however, the vector $\mathbf{w}=\mathbf{k}-\mathbf{q}$ to be different from zero. We study both small values of $w \lesssim 1.5$ fm^{-1} and rather large values of w up to about 4 fm^{-1} which corresponds to about 800 MeV/c.

In Fig. 2 we show the moduli of the transition form factors for the s-wave bound state in the square well potential. Two cases, $k=q=2$ and 4 fm^{-1}, are shown. As expected the plane-wave form factor (5) falls down quickly with w (power law decrease[4]). Both the exact and approximate form factors display a much slower falloff for large values of w (see also Fig. 3). The on shell approximation (27), which underestimates the form factor, especially for small values of w, and displays a too diffractive pattern, seems rather inappropriate, at least in the momentum range considered here. We shall not comment further on this approximation. As far as the eikonal approximation (28) is concerned we observe (Figs. 2 and 3) that it underestimates the transition form factor in the region $w \lesssim 1$ fm^{-1}. In the region $w \gtrsim 1$ fm^{-1} one notes a large increase as compared to the plane-wave result. Comparing, however, to the exact calculation, the FSI is obviously underestimated and the (too) diffractive pattern is shifted towards larger values of w. As expected, we have checked that for larger values of k (i.e., $k \simeq 4$ fm^{-1}), the eikonal results get closer to the exact ones and have the correct qualitative behavior.

We now come to the comparison of the exact form factor (21) and the approximate one as given by Eqs. (7) and (19). We note a qualitative agreement which becomes quantitative ($k=q=4$ fm^{-1}) as the energy of the ejected nucleon increases. At small values of $w \lesssim 1$ fm^{-1} the final state interaction reduces the plane-wave form factor by about 30% at $k=q=2$ fm^{-1} and about 8% at 4 fm^{-1}. This situation is completely reversed for $w > 1.5$ fm^{-1} where the distortion of the nucleon wave leads to the remarkable *increase* of the transition amplitude. This behavior has to be related to multiple scattering contributions in this region. Indeed it does not require high Fourier components of the bound state wave function to realize a momentum transfer, w, of the order of 3 to 4 fm^{-1} by successive collisions at small momentum transfers, whereas a direct knockout at such large w, is strongly suppressed as indicated by the plane-wave calculation. Rescattering must at the same time lead to a suppression in the small w region. The reduction of FSI as the energy increases is easily understood in terms of a perturbative expansion.

The region k of the order of 3 to 4 fm^{-1} is therefore suitable for exploring the nuclear structure properties[13] over a wide range of nucleon momenta (Fermi motion). It is sensitive not only to the nuclear radius[12] but also to the diffuseness of the potential well. This effect is shown in Fig. 4 where similar curves are plotted for the Woods-Saxon potential. The influence of the potential diffuseness is most effective for $w > 1.5$ fm^{-1} where the transition form factor decreases much faster (exponentially, as shown in Ref. 3) than the corresponding square well form factor. On the other hand for the small w values its

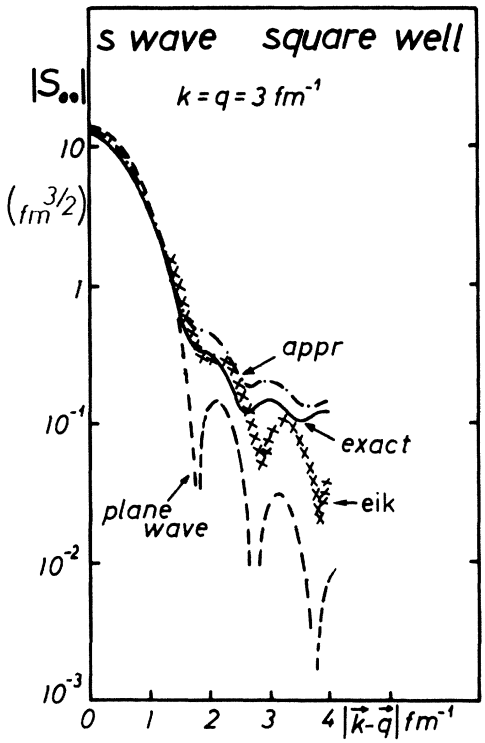

FIG. 3. Same as Fig. 2 but for $k=q=3$ fm^{-1}. The on shell approximation has been omitted (27).

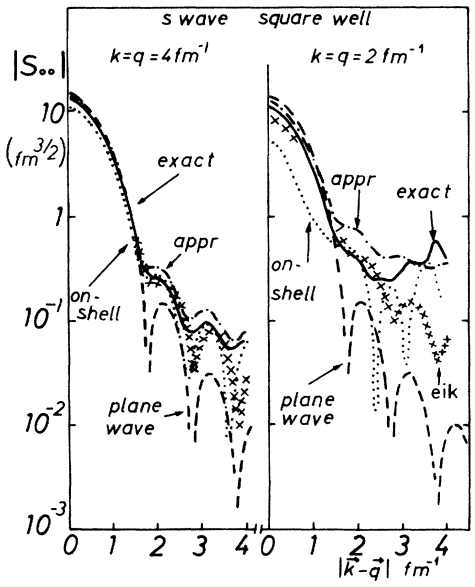

FIG. 2. Absolute value of the s-wave transition form factor for the square well potential for $k=q=2$ fm^{-1} and $k=q=4$ fm^{-1}. The solid lines correspond to the exact calculation (21) while the dashed-dotted lines correspond to the approximate results (7) and (19), the dashed line to the plane-wave contribution (5). The dotted line shows the results of the on shell approximation (27) and the crosses represent the eikonal approximation (28).

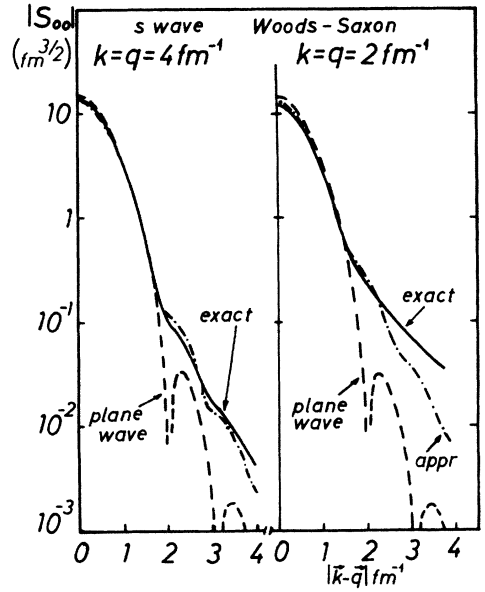

FIG. 4. Same as Fig. 2 but for the Woods-Saxon potential (30).

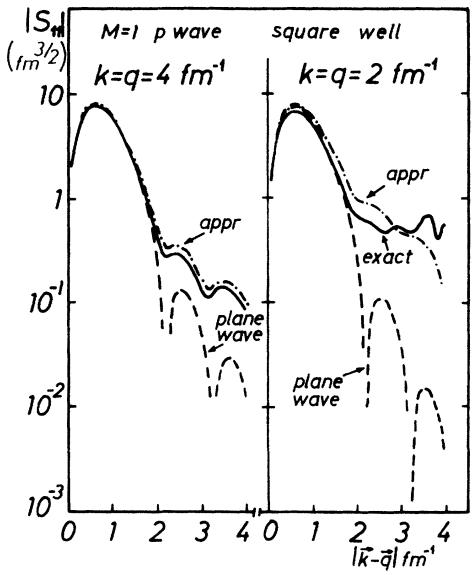

FIG. 6. Same as Fig. 5 but for the $M=1$ projection.

behavior is dominated by the plane-wave contribution and it is not changed very much in comparison with the square well case.

For the p-wave bound state, the transition form factors corresponding to the three eigenstates of the spin projection quantum number $M=0$ or ± 1 have a completely different pattern. In Fig. 5 we see the remarkable difference between the plane-wave curve going to zero in the $\mathbf{k}-\mathbf{q}=0$ limit and the finite values of the exact and approximate form factors which for $M=0$ have a maximum there. This maximum exists also for higher momentum $k=4$ fm^{-1} although its value is decreased in comparison with the smaller momentum case. Figure 6 shows the results for the $M=1$ projection on the q axis. Now all the curves tend to zero for vanishing w. The $M=-1$ case leads to the same figure as the $M=1$ case. We also calculate the overall p transition form factor squared

$$S_p^2=\tfrac{1}{3}(|S_{10}|^2+|S_{11}|^2+|S_{1-1}|^2) \tag{31}$$

for the square well (Fig. 7) and for the Woods-Saxon case (Fig. 8). As a general remark concerning the p-wave bound state case, since the plane wave has a zero for

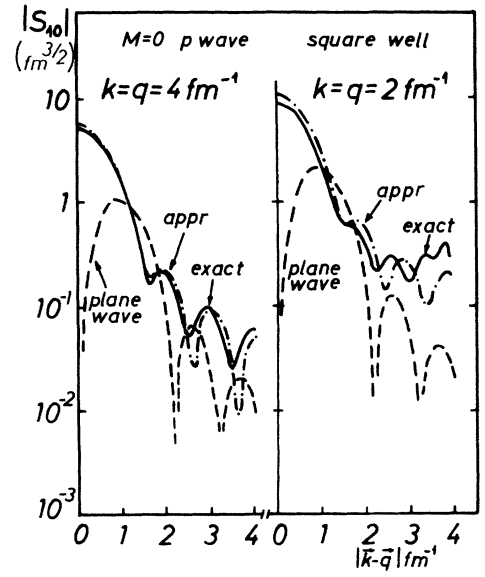

FIG. 5. Spin projection $M=0$ p-wave transition form factor for the square well potential (the quantization axis is chosen along the momentum transfer, $\mathbf{q}$, direction). The exact (solid line), approximate (dashed-dotted line), and plane-wave (dashed line) results are displayed.

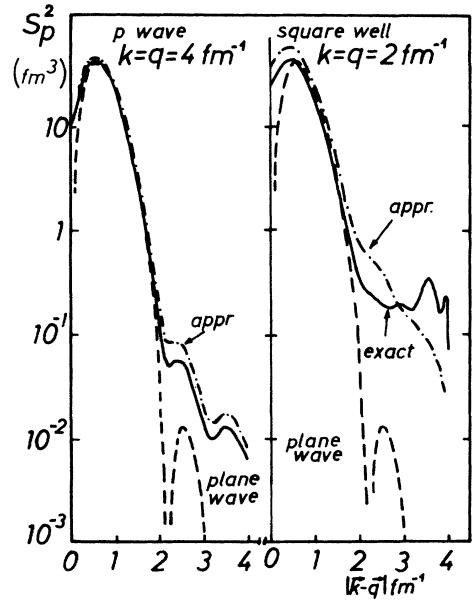

FIG. 7. Same as Fig. 5 but for the averaged p-wave transition form factor (31).

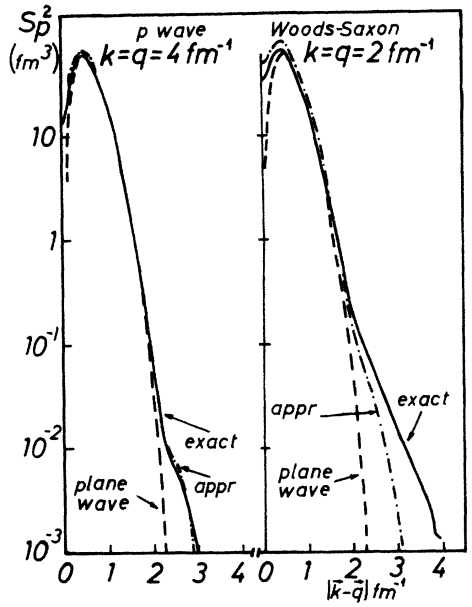

FIG. 8. Same as Fig. 7 but for the Woods-Saxon potential (30).

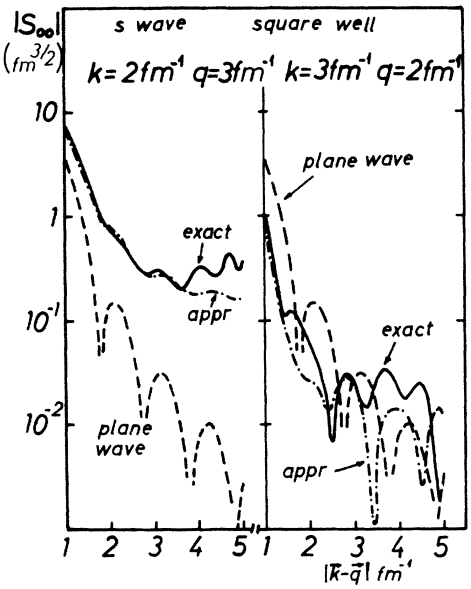

FIG. 9. Same as Fig. 2 but for $k=2$ fm^{-1}, $q=3$ fm^{-1} and $k=3$ fm^{-1}, $q=2$ fm^{-1}.

$w=0$, the plane-wave approximation necessarily fails in the small w region (i.e., $w \lesssim 0.5$ fm^{-1}). We stress that Figs. 2–8 correspond to the quasifree kinematics regime $k=q$.

The approximation (19) to the transition form factors yields a good agreement with the exact calculation at the higher energies. Even for large values of w the difference between the exact and approximate form factors remain at the level of 25%. The effective Green's function introduced in evaluating the correction (8) (see Refs. 3 and 4) therefore provides a reasonable approximation which takes into account at the same time binding corrections and rescattering contributions. At lower energies (i.e., $k=2$ fm^{-1}) it still gives a semiquantitative agreement with the exact calculation. As expected, the results for a smooth potential (30) are in closer agreement with the exact calculation than for the sharp cutoff potential (29).

Other cases namely $k<q$ or $k>q$ are also interesting. In Fig. 9 the two sets of curves $k=2$, $q=3$ fm^{-1} and $k=3$, $q=2$ fm^{-1} refer to the knockout from a s-wave bound state in a square well potential. In the first case ($k<q$) the plane-wave curve lies *below* the exact one, while in the second case it lies *above*, indicating a destructive interference between the plane-wave amplitude and rescattering contribution, at least for not too large values of w. Since the plane-wave results are identical in both cases, it is the attractive nature of the potential which binds the nucleon in the initial state and is also responsible for the FSI which leads to the enhancement of the transition probability for the case $k<q$. The same holds true for the p wave as illustrated in Figs. 10 and 11. For the s wave, also noticeable is the good agreement of approximation (19) with the exact calculation (particularly for $k<q$), even for relatively large values of w (i.e., away from the quasifree kinematics) and in the presence of strong FSI (e.g., $k=2$ fm^{-1}). Although we do not illustrate the results for large k's, it is clear that the agreement is even better.

Figure 10 is similar to Fig. 9 but for the Woods-Saxon potential. The main effect of the diffuseness is to suppress the large w contributions revealing less high momentum components in the ground state wave function due to the absence of a sharp edge.

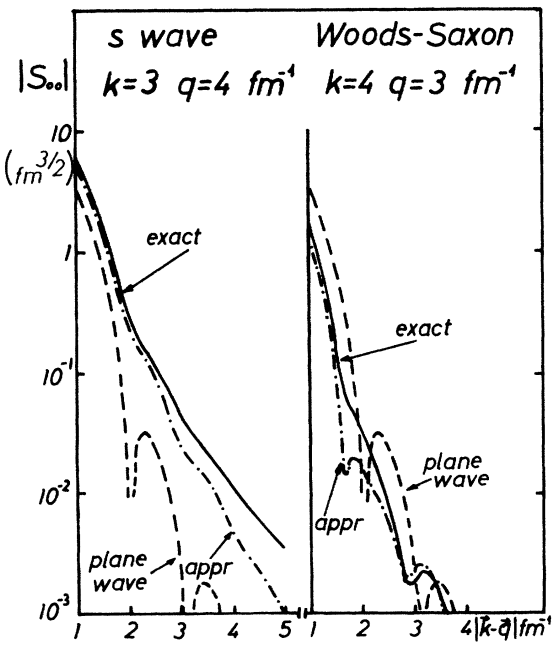

FIG. 10. Same as Fig. 9 but for $k=3$ fm^{-1}, $q=4$ fm^{-1} and $k=4$ fm^{-1}, $q=3$ fm^{-1} and for the Woods-Saxon potential (30).

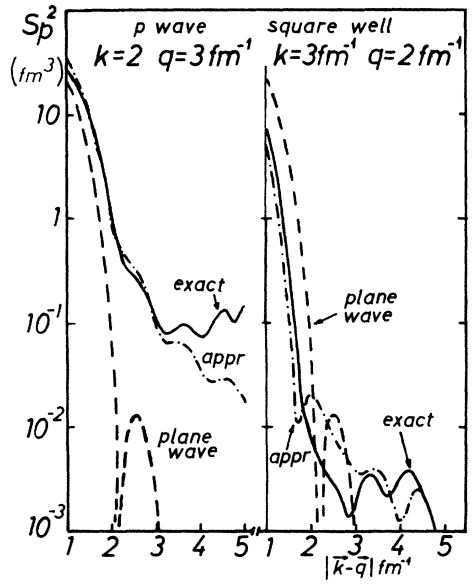

FIG. 11. Same as Fig. 7 but for $k=2$ fm^{-1}, $q=3$ fm^{-1} and $k=3$ fm^{-1}, $q=2$ fm^{-1}.

IV. SUMMARY AND DISCUSSION

We have investigated the FSI effects for the transition form factor for a nucleon knockout reaction. This form factor may be represented as a function of $|\mathbf{k}-\mathbf{q}|$ for a given momentum transfer of the probe, $\mathbf{q}$, and a given asymptotic momentum, $\mathbf{k}$, of the ejected nucleon. Clearly the small $|\mathbf{k}-\mathbf{q}|$ region is a little sensitive to FSI effects; at the same time, however, it is barely sensitive to the details of the nucleon bound state wave function. In that regime, $|\mathbf{k}-\mathbf{q}| \lesssim 1$ fm^{-1}, the plane-wave approximation to the form factor provides an almost quantitative agreement with the exact calculation. It is only in a region starting around $|\mathbf{k}-\mathbf{q}| \simeq 2$ fm^{-1} that the form factor becomes sensitive to the shape of the nuclear potential. The influence of the diffuseness of the nuclear surface is quite important as the comparison between the square well and Woods-Saxon potentials shows (about one order of magnitude between the two calculations for $|\mathbf{k}-\mathbf{q}|$ around 2.5 fm^{-1}). In that region, however, the role of the final state interaction is already important (except for unduly large values of the asymptotic energy of the ejected nucleon for which relativistic effects would have to be incorporated).

We have also, at that stage, studied the role of the unphysical discontinuity of the first derivative of the Woods-Saxon potential at the origin; it leads to an asymptotic power falloff of the momentum space wave function following an intermediate exponential falloff regime. We have therefore redone calculations using the symmetric form

$$V(r)=-\frac{V_0}{2}\left[\tanh\left[\frac{r+c}{2\beta}\right]-\tanh\left[\frac{r-c}{2\beta}\right]\right] \quad (32)$$

with V_0, c, and β defined as before. Such a form is similar to those used in Refs. 14. This form leads to an exponential asymptotic behavior in momentum space. In the range of momenta studied here, there are no differences whatsoever between the two calculations. The onset of the power falloff regime starts at larger values of $|\mathbf{k}-\mathbf{q}|$. This could be expected since the differences between (30) and (32) are only significant in the extreme interior region.

One of the main conclusions of the present study, within the framework of a very simple model, is that a very careful treatment of FSI is necessary if one wants indeed to extract information on nuclear structure, such as on momentum distributions, from knockout reactions. The appropriate regime in which one may hope to investigate nuclear structure information seems to be around $|\mathbf{k}-\mathbf{q}| \gtrsim 2$ fm^{-1} for ejected nucleon momenta, k, between 2 and 4 fm^{-1}. Larger k, within this regime, have the advantage of minimizing the role of FSI.

We have compared various treatments of FSI which yield answers quickly far off the results of an exact calculation. It is only within the approximation (19), proposed in Ref. 3, that we could obtain a good agreement with the corresponding exact calculations. This approximation can therefore provide a meaningful starting point for this sort of investigation. Let us remind one, at this stage, that in the context, the approximate transition form factor is evaluated from the knowledge of the bound state wave function and of the potential only. It can be conveniently evaluated numerically through a partial wave expansion. We remark that the plane-wave approximation can, in no case, bring a satisfactory evaluation of the form factor, even if renormalized, if one considers a momentum range larger than 2 fm^{-1}.

As a result of the numerical calculation discussed in Sec. III we note that approximation (19) is particularly good when the energy of the ejected nucleon is large. This has to be expected since (19) has been developed as a high energy approximation.[3,4] This approximation is best when the ejected nucleon momentum, k, matches the momentum, q, brought in by the probe. We have remarked that, away from the quasifree kinematics regime, the approximation (19) provides a fairly good agreement with the exact calculation, particularly for k less than q. This is explained by the fact that the role of the high momentum components of the bound state wave function is less relevant then that in the opposite situation, i.e., $k>q$. On the other hand we know that, in the extreme limit when q is very much smaller than k, where the role of the high Fourier components of the wave function is maximized, the approximation (19) has been shown to fulfill the orthogonality requirement.[4]

One should remember that our results here have been derived within a naive one-body picture for the description of the initially bound nucleon. Yet it is well known that short-range correlations, even in a plane-wave treatment of the final state, would yield deviations from the plane-wave shell model calculation because of the enhancement of the high Fourier components of the bound state wave function. Such deviations would be similar to those arising from FSI (see, for instance, Ref. 6); the falloff at large $|\mathbf{k}-\mathbf{q}|$ becomes much less pronounced than in a plane-wave calculation. It is not at all

clear whether there is a kinematical region where the effects of short-range correlations and those due to FSI could be separated. The most likely answer to such a question is probably negative. Yet, it would be interesting to explore experimentally the region suggested above. At this time, to our knowledge, no systematic (e,e'p) data exist in this domain. Specific (i.e., perpendicular, for instance) kinematical configurations should facilitate the qualitative understanding of asymmetries of the nucleon momentum distributions[6] which are sensitive to the details of the nucleon-nucleus interaction like the spin orbit contribution. For sufficiently large energies of the ejected nucleon, high energy approximations similar to that studied here [see Eq. (19)] or, even, the eikonal approximation should be useful in such studies.[15]

A realistic treatment of such reactions requires a many-body approach. It is not clear how a practical calculation starting from similar approximations to those leading to Eqs. (8) and (19) could be performed for the real many-body problem. The standard approach would be to generate FSI via an energy dependent complex optical potential in the context of a DWIA analysis. In such a framework, one could think of deriving an approach similar to that developed in the present work by assuming that the optical potential has the same radial dependence as the bound state potential. However the effective Green's function which enters Eqs. (11) or (13) will also be modified. The real part of the optical potential would be weaker than the binding potential and less attraction will result but part of the strength will be redistributed via the imaginary part. Moreover the consistency requirement provided by the orthogonality constraint is then lost and it is very difficult to judge how the present results would be modified in such an analysis. In our opinion a theoretical calculation using a coupled channel formalism, as in Ref. 2, could be performed using approximations similar to those developed here.

ACKNOWLEDGMENTS

One of us (F.C.) is grateful to the Division de Physique Théorique of the Institute de Physique Nucléaire at Orsay, as well as to the University Paris VII for hospitality and support. L.L. would like to thank Istituto Nazionale di Fisica Nucleare at Bologna and the Institut de Physique Nucléaire at Orsay for the hospitality extended to him during the visits at both institutes where part of this work has been accomplished. Finally we have appreciated the help of G. Fratamico in some of the calculations presented here. This work has been supported in part by the M. Sklodowska-Curie Foundation, Grant No. F7-071-P. The Division de Physique Théorique is a laboratory associated with Centre National de la Recherche Scientifique.

---

*Mailing address: Division de Physique Théorique, Institut de Physique Nucléaire, B.P. 1, F-91406 Orsay, Cedex, France.

[1]F. Cannata, J. P. Dedonder, and F. Lenz, Ann. Phys. (N.Y.) **143**, 84 (1982).

[2]Q. Haider and J. T. Londergan, Phys. Rev. C **23**, 19 (1981).

[3]F. Cannata, J. P. Dedonder, and S. A. Gurvitz, Nuovo Cimento **76A**, 478 (1983); Phys. Rev. C **27**, 1697 (1983).

[4]R. D. Amado, F. Cannata, and J. P. Dedonder, Phys. Rev. C **31**, 162 (1985).

[5]R. D. Amado and R. Woloshyn, Phys. Lett. **69B**, 400 (1977).

[6]S. Frullani and J. Mougey, *Advances in Nuclear Physics,* edited by J. W. Negele and E. Vogt (Plenum, New York, 1985), Vol. 15.

[7]A. R. Edmonds, *Angular Momentum in Quantum Mechanics* (Princeton University, Princeton, N.J., 1957).

[8]M. Abramowicz and I. A. Stegun, *Handbook of Mathematical Functions* (Dover, New York, 1972).

[9]K. M. Watson, Phys. Rev. **95**, 228 (1954).

[10]See for instance J. N. Ginocchio, Phys. Rev. C **17**, 195 (1978) or Y. Yariv and Z. Fraenkel, *ibid.* **20**, 2227 (1979).

[11]J. Noble, Phys. Rev. C **17**, 2151 (1978); see also J. M. Eisenberg, Ann. Phys. (N.Y.) **71**, 548 (1972); J. R. Shepard and E. Rost, Phys. Rev. C **25**, 2660 (1982).

[12]Since the radii of both the square well and the Woods-Saxon potentials have been fixed to the value $c=3$ fm, the bound state wave functions radii are slightly different. The minima in the transition form factors are therefore slightly shifted in the corresponding calculations.

[13]In a more phenomenological calculation, this energy domain, corresponding to $k\approx 3$ to 4 fm^{-1}, should be relevant for the study of nuclear structure since the elementary interaction is comparatively weak. If one looks at the proton-proton and proton-neutron total cross sections as functions of the laboratory momentum, one finds that their minima are in the region of k from about 3 to 4 fm^{-1} ($\sigma^{pp}_{min}\approx 22$ mb and $\sigma^{pn}_{min}\approx 32$ mb). Particle Data group, Rev. Mod. Phys. **56** (1984), No. 2, part 2; H. Spinka, Proceedings of the 1984 Workshop on Nuclear Physics with Stored Cooled Beams, University of Indiana, 1984; P. W. Lisowski *et al.*, Phys. Rev. Lett. **49**, 255 (1982).

[14]V. V. Burov, Yu, N. Eldyshev, V. K. Lukyanov, and Yu. S. Pol, Joint Institute of Nuclear Research, Dubna Report E4-8029, 1974; B. Buck and A. A. Pilt, Nucl. Phys. **A280**, 133 (1977).

[15]F. Cannata, J. P. Dedonder, and J. R. Gillespie (unpublished).